ARTICLE

Measurement of the Optical Properties and Shape of Nanoparticles in Solution Using Couette Flow

John E. Sader,[†] Christopher J. Pepperell,[†,‡] and Dave E. Dunstan[‡,*]

[†]Department of Mathematics and Statistics and [‡]Department of Chemical and Biomolecular Engineering, University of Melbourne, Victoria, 3010, Australia

ABSTRACT Knowledge of the optical properties and shape of nanoparticles is central to many technological applications including the fabrication of advanced materials and the characterization and formation of ordered films for optoelectronic devices. Measurement of such properties typically involves the independent use of advanced instrumentation such as electron and near field optical microscopy. We propose a simple experimental technique for extracting the optical and geometric properties of dilute suspensions of nanoparticles *in situ*. A theoretical formalism is developed to determine both the dichroic ratio and aspect ratio from a single measurement of the change in extinction of an incident light beam. The validity of this method is demonstrated for hematite nanorods, for which good agreement with independent measurements is found.

KEYWORDS: nanorods · anisotropic optical properties · Couette flow · Jeffrey orbits · dilute suspensions

Fabrication of nanostructured materials often relies on ability to process nanoparticles, quantum dots, and macromolecules into ordered macroscopic arrays[1] with the underlying chemical, mechanical, and optical properties of these advanced materials being dictated by the primary properties of their constituents. Determination of the optical properties of small particles, in particular, has received considerable attention from both a theoretical and experimental perspective, due to the relative ease in which they can be tuned at the nanoscale.[2] Of primary interest in many studies has been the strong effect of geometry and proximity to surfaces on the optical properties of nanoparticles.[2] As such, ability to measure and manipulate the shape of small particles is fundamentally important in controlling the global optical and electronic behavior of bulk nanostructured materials.[3]

Independent techniques, such as electron and near-field optical microscopy, are normally required to measure both the optical and geometric properties of nanoscale materials. The aim of this article is to propose a simple *in situ* method that circumvents this requirement and allows for the simultaneous measurement of both the hydrodynamic aspect ratio and dichroic ratio of a dilute dispersion of small particles. This is particularly relevant in practice, since wet chemistry techniques are often used to synthesize nanoparticles in solution.

With an optical Couette flow cell (see Figure 1), the polarized UV–vis absorption spectra of a dilute system of particles is interrogated and analyzed. A related type of experimental setup has previously been the basis for birefringence, dichroism, fluorescence, light scattering, and neutron scattering techniques.[4] In ref 5, a rheooptic technique was proposed to measure the particle aspect ratio from transient time-dependent measurements of the particle orientation. In contrast, the present technique relies solely on steady-state (time-independent) measurements, thus significantly simplifying implementation. The optical Couette cell described here is developed to measure the absorbance of polarized light as a function

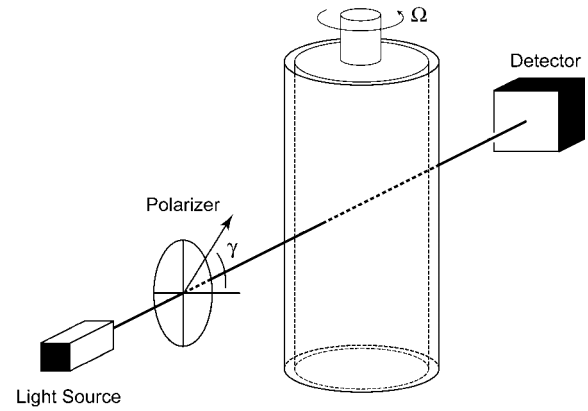

Figure 1. Schematic of optical Couette flow apparatus.

*Address correspondence to davided@unimelb.edu.au.

Received for review October 17, 2007 and accepted January 16, 2008.

Published online February 9, 2008.
10.1021/nn700304b CCC: $40.75

of flow rate and polarization angle. Both the dichroic ratio and hydrodynamic aspect ratio of the particles are interpreted simultaneously from the data. This is achieved through development of a simple (analytical) theoretical formalism that accounts for both the motion of the particles and their optical properties. Interestingly, we establish that the polarization angle giving zero change in optical extinction of the flowing dispersion of particles is not connected to the particle dichroic ratio but is a function of the particle hydrodynamic aspect ratio only. This unintuitive finding has obvious implications to previous measurements that rely on the point of zero change in extinction for determination of the dichroic ratio.[6] Results obtained for a dilute particulate dispersion in flow[7] are presented and shown to be in good agreement with known properties of this system.

The optical Couette flow cell[6,7] consists of two concentric cylinders whose radii greatly exceed the gap distance. As such, the flow between the cylinders represents a simple Couette shear flow. A light beam is incident normal to the cylinder surfaces (see Figure 1). The fluid within the Couette flow cell is the (infinitely) dilute dispersion of particles. In a quiescent state, this ensemble of particles will take all orientations randomly since the particles are noninteracting due to infinite dilution. As the shear rate increases the particles begin to respond by orienting with the flow field, and the magnitude of incident light absorbed by the particles changes. We consider the case where the applied flow field dominates the Brownian motion of the particles, corresponding to the high Peclet number limit. Below we derive a theoretical model that relates the optical extinction of the incident light beam to the applied shear field.

Since the dispersion of particles is dilute, we are able to examine the behavior of each particle individually. We consider an axisymmetric rodlike particle such as a spheroid; see Figure 2. The principal optical axis of the particle is assumed to coincide with its principal geometric axis.[8] The absorption cross sections along each geometric axis of the particle are defined to be A_1, A_2, and A_3, with the 1-direction corresponding to the long axis. It is assumed that absorbance along the minor axes in the 2- and 3-directions are identical, *i.e.*, $A_2 = A_3$. We note that as the particle size approaches the dipole limit, the absorption cross sections can be defined in terms of components of optical polarizability (α_1, α_2, α_3) relating to the transition dipole moment of the particle. In this special case, $A_n = k\,\mathrm{Im}\{\alpha_n\}$ where $n = 1$, 2, or 3 and k is the wavenumber. Nonetheless, here we consider in complete generality the case where the particle is of arbitrary size, provided the principal optical absorption axes correspond to the principal geometric axes of the particle. In a quiescent state, the particles are randomly oriented and the net absorption cross section of the ensemble is simply given by $\langle c_{abs}\rangle = (A_1 + 2A_2)/3$, regardless of the polarization of the incident light.

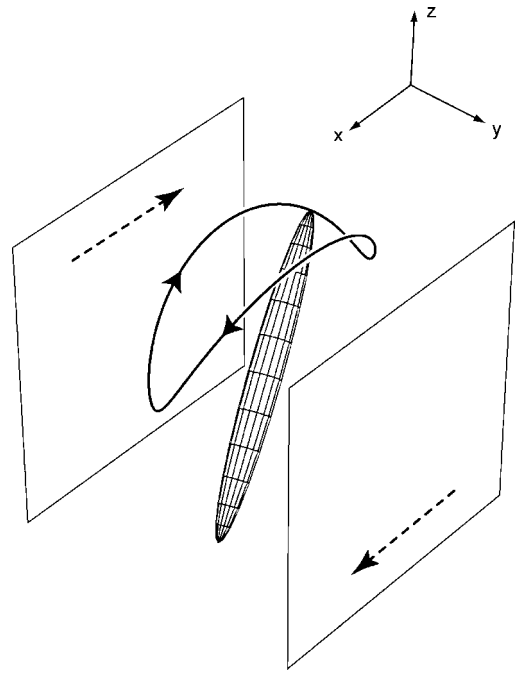

Figure 2. Schematic of the Jeffery orbit of a particle in shear flow. Cartesian coordinate system is indicated.

Jeffery[9] has shown that rodlike particles in simple shear flow undergo periodic orbits. These so-called Jeffrey orbits are strongly dependent on the initial position of the particle. Considering motion relative to the particle center of mass, it is observed that the particle follows a trajectory similar to the orbit shown in Figure 2. For increased geometric aspect ratio (length along major axes relative to minor axis), the time spent aligned in the shear direction relative to the orbit period increases. Importantly, all particles possessing geometric axisymmetry undergo such Jeffrey orbits in shear flow, and their motion relative to a spheroid can be related through an effective "hydrodynamic aspect ratio".[10] As such, analysis of a spheroid can be applied directly to axisymmetric particles of arbitrary shape through an appropriate choice of hydrodynamic aspect ratio.[10]

The angles θ and φ are used to specify the particle orientation. The origin of the coordinate system is taken at the center of mass of the particle. As such, θ specifies the angle between the major axis of the particle and the z-axis, whereas φ gives the angle specified by the projection of the major axis of the particle on the $x-y$ plane relative to the y-axis; see Figure 2. These two angles thus uniquely specify the orientation of the major axis of the particle in the flow field. The Jeffrey orbits[9] of the particle are given by the equations

$$\tan\theta = C\sqrt{\cos^2\tau + r_e\sin^2\tau} \qquad (1)$$

$$\tan\varphi = r_e\tan\tau$$

where $\tau = 2\pi t/T + \kappa$, t is time, r_e is the hydrodynamic aspect ratio of the particle, the period of oscillation is given by $T = (2\pi/G)(r_e + r_e^{-1})$ and G is the shear rate of the imposed flow field. Importantly, the coefficients C and κ specify the initial orientation of the particle; an orbit constant $C = 0$ corresponds to the rod permanently aligned with the z-axis, whereas $C \gg 1$ indicates that the rod is aligned in the $x-y$ plane. The effect of the Jeffrey orbits on the optical absorbance can then be calculated by suitably averaging over all initial orientations of the particle since we are considering an ensemble of particles.

Leal and Hinch[11] noted that the intuitive assumption of initial random particle orientation (the so-called Eisenschitz condition[12]) does not always apply to particles undergoing Jeffrey orbits at high Peclet numbers, due to the singular nature of this limit. Following Leal and Hinch,[11] the governing equation for the orbital distribution function $f(C)$ is given by

$$[H(r_e)C^4 + K(r_e)C^2 + M(r_e)]\frac{df}{dC} + \frac{1}{C}[2H(r_e)C^4 + (6 - K(r_e))C^2 - M(r_e)]f = 0 \quad (2)$$

where $H(r_e) = r_e^2 + 1$, $K(r_e) = r_e^2/4 + 7/2 + 1(4r_e^2)$, and $M(r_e) = 1 + r_e^{-2}$. For comparison, the corresponding result for the (random) Eisenschitz condition is given explicitly as

$$f(C) = \frac{Cr_e}{2\pi^2\sqrt{1 + C^2}(1 + r_e^2C^2)}E\left(\frac{C^2(1 - r_e^2)}{C^2 + 1}\right) \quad (3)$$

where $E(m)$ is the complete elliptic integral.[13] Importantly, the orbital distribution function for the Eisenschitz condition only differs considerably from that of Leal and Hinch when the particle is aligned close to the vorticity axis (small C) when the aspect ratio r_e is considerably greater than unity, the effect of which will be discussed below.

Since the incident light is perpendicular to the surface of the Couette flow cell, we need only consider the absorption cross sections of the particles in the x- and z-directions; see Figure 2. As the particles move in their Jeffrey orbits, the absorption cross section of the particles varies. However, since a large number of orbits are sampled, the absorption measurements are only sensitive to the time-averaged absorption cross section. To calculate this average, we first express the particle absorption cross sections relative to fixed Cartesian coordinate system (as in Figure 2), yielding

$$c_{abs,x} = A_1 \sin^2\theta \sin^2\varphi + A_2(\cos^2\varphi + \cos^2\theta \sin^2\varphi) \quad (4a)$$

$$c_{abs,z} = A_1 \cos^2\theta + A_2 \sin^2\theta \quad (4b)$$

The average absorption cross section in the x- and z-directions is then obtained by taking the time-averaged absorption cross section of the particle as it moves through each Jeffrey orbit and the weighted average over the distribution of Jeffrey orbits specified above. Expressed in C and τ space of the Jeffrey orbits, this leads to the following result

$$\langle c_{abs,i}\rangle = 2\int_0^\infty \int_0^{2\pi} f(C)c_{abs,i}\, d\tau\, dC \quad (5)$$

where i takes on x and z. Substituting the expressions for the Jeffrey orbits defined in eqs 1–3 into eq 4 and subsequently eq 5, then enables the average absorption cross section in the x- and z-directions to be calculated. The resulting extinction coefficient as a function of polarization angle γ relative to the z-axis is then immediately determined from

$$\epsilon(\gamma) = n_p(\langle c_{abs,x}\rangle \cos^2\gamma + \langle c_{abs,z}\rangle \sin^2\gamma) \quad (6)$$

where $\langle c_{abs,x}\rangle$ and $\langle c_{abs,z}\rangle$ are the average absorption cross sections in the x- and z-directions, respectively, γ is the polarization angle defined in Figure 1, and n_p is the total number of particles sampled by the incident light. All measurements of the extinction coefficient are taken relative to the quiescent state (zero shear), whose extinction coefficient is defined as $\epsilon_0(\gamma)$.[14] Therefore, the change in extinction coefficient $\Delta\epsilon(\gamma)$ relative to the quiescent state can be expressed generally as

$$\Delta\epsilon(\gamma) \equiv \epsilon(\gamma) - \epsilon_0(\gamma) = \beta_1 \cos^2\gamma - \beta_2 \sin^2\gamma \quad (7)$$

where the coefficients β_1 and β_2 are the change in extinction values at 0 and 90° polarization angles.

Infinite Hydrodynamic Aspect Ratio. We now examine the limiting case where the hydrodynamic aspect ratio of the particle $r_e \to \infty$. In this singular limit, the particle spends all its time aligned in the flow direction, for which we obtain $\langle c_{abs,x}\rangle = A_1$ and $\langle c_{abs,z}\rangle = A_2$. Combining this with the result for a quiescent fluid, then yields

$$\beta_1/\beta_2 = 2 \quad (8)$$

regardless of the values of A_1 and A_2. This result establishes that the angle of zero change in extinction, $\Delta\epsilon = 0$, is independent of the optical properties of the particle provided the hydrodynamic aspect ratio r_e greatly exceeds unity. The implications of this finding will be discussed below.

Next, we determine the relationship between the extinction coefficients when the light is unpolarized.[14] In this case, the particles can be considered to be randomly oriented in the $x-z$ plane, for which the absorption cross section is given by $\langle c_{abs}\rangle_{2D} = (A_1 + A_2)/2$. The subscript 2D is used to indicate that the particles

are in a flow field and oriented in the $x-z$ plane, whereas 3D is used for the quiescent state (no flow). Consequently, for the case of unpolarized light, the ratio of the absorption cross sections of the flowing dispersion relative to the quiescent dispersion is given by

$$\frac{\langle c_{abs}\rangle_{2D}}{\langle c_{abs}\rangle_{3D}} = \frac{3}{2}\left(\frac{1+(A_2/A_1)}{1+2(A_2/A_1)}\right) \quad (9)$$

We find that the ratio of these absorption cross sections depends on the dichroic ratio A_2/A_1 and varies between 3/2 (for the uniaxial case $A_2 = 0$) to 3/4 (for the biaxial case $A_1 = 0$).

Finite Hydrodynamic Aspect Ratio. We now examine how the ratios β_1/β_2 and $\langle c_{abs}\rangle_{2D}/\langle c_{abs}\rangle_{3D}$ depend on the hydrodynamic aspect ratio r_e using the formalism specified above. We focus on the case corresponding to rodlike particles with $r_e > 1$. Given the analytical complexity of the above formalism, derivation of exact analytical formulas for β_1/β_2 and $\langle c_{abs}\rangle_{2D}/\langle c_{abs}\rangle_{3D}$ poses a formidable challenge. The aim here is therefore to derive approximate yet accurate analytical formulas that can be used to interpret experimental measurements. This is achieved by first taking the Taylor series expansion of the orbital distribution function $f(C)$ with respect to r_e about $r_e = 1$. The integral specified in eq 5 is subsequently evaluated analytically to yield a Taylor series expansion about $r_e = 1$ of the absorption cross sections in the x- and z-directions. The results for β_1/β_2 and $\langle c_{abs}\rangle_{2D}/\langle c_{abs}\rangle_{3D}$ are then calculated, yielding the following asymptotic series expansions for the Leal and Hinch[11] condition:

$$\frac{\beta_1}{\beta_2} = \frac{7}{2(r_e-1)} + \frac{9}{4} - \frac{107}{792}(r_e-1) + O(r_e-1)^2 \quad (10a)$$

$$\frac{\langle c_{abs}\rangle_{2D}}{\langle c_{abs}\rangle_{3D}} = 1 + \Delta A\left(\frac{3}{10}(r_e-1) - \frac{27}{140}(r_e-1)^2 + \frac{23}{175}(r_e-1)^3\right) + O(r_e-1)^4 \quad (10b)$$

where $\Delta A = (A_1 - A_2)/(A_1 + 2A_2)$. Note that the expansions for the Eisenschitz[12] condition are very similar

$$\frac{\beta_1}{\beta_2} = \frac{7}{2(r_e-1)} + \frac{9}{4} - \frac{3}{88}(r_e-1) + O(r_e-1)^2 \quad (11a)$$

$$\frac{\langle c_{abs}\rangle_{2D}}{\langle c_{abs}\rangle_{3D}} = 1 + \Delta A\left(\frac{3}{10}(r_e-1) - \frac{27}{140}(r_e-1)^2 + \frac{9}{70}(r_e-1)^3\right) + O(r_e-1)^4 \quad (11b)$$

with deviations occurring only in the higher order terms. For β_1/β_2, deviations between the Eisenschitz and the Leal and Hinch formulations occur in the third term, whereas for $\langle c_{abs}\rangle_{2D}/\langle c_{abs}\rangle_{3D}$ they occur in the fourth term. This finding together with the corresponding result for $r_e \to \infty$ indicates that the solution for arbitrary r_e is very weakly dependent on the choice of orbital distribution function.

To complete the formulation, we now construct uniformly valid formulas from the above asymptotic results. We again note the important result that the ratio β_1/β_2, which is obtained from optical absorption measurements along the x- and z-directions, is independent of the optical properties of the rod and depends only on its shape through the hydrodynamic aspect ratio r_e. Noting the corresponding limits for $r_e = 1$ and $r_e \to \infty$ leads to the following uniformly valid result for β_1/β_2

$$\frac{\beta_1}{\beta_2} = 2 + \frac{7}{2(r_e-1)} + \frac{1}{4r_e} \quad (12)$$

The first two terms in this expression are obtained directly from the leading order asymptotic behavior for $r_e \to 1$ and $r_e \to \infty$, whereas the third term is obtained by ensuring that the second order behavior in the $r_e = 1$ asymptotic series in eq 10a is fulfilled.

The corresponding result for $\langle c_{abs}\rangle_{2D}/\langle c_{abs}\rangle_{3D}$ is obtained by using the first two terms in eq 10b together with the limiting behavior as $r_e \to \infty$ to construct a Padé approximant that satisfies both limits as $r_e \to 1$ and $r_e \to \infty$. This gives the following uniformly valid solution

$$\frac{\langle c_{abs}\rangle_{2D}}{\langle c_{abs}\rangle_{3D}} = \frac{10 + 9\left[\frac{1+(A_2/A_1)}{1+2(A_2/A_1)}\right](r_e-1)}{10+6(r_e-1)} \quad (13)$$

Equations 12 and 13 are the results we seek and enable the dichroic ratio A_2/A_1 and hydrodynamic aspect ratio r_e of the particle to be determined from measurements of the extinction coefficient under flow and in a quiescent state.

Importantly, eqs 12 and 13 exhibit excellent agreement with the full exact solution for both the Eisenschitz and the Leal and Hinch conditions, as illustrated in Figure 3. Note that the use of these different criteria has little effect on the overall result, as expected. Consequently, these formulas can be used in confidence in place of the full (numerical) solutions.

A schematic diagram of the Couette cell is shown in Figure 1. The cell is mounted in the beam of a UV–vis spectrometer (Cary 3E) operating at $\lambda = 392$ nm wavelength as described previously.[6] The incident beam was polarized using a Melles Griot Glan-Thompson polarizer. The angle of polarization was adjusted manually ($\pm 0.5°$). Baseline calibration was performed using a zero shear rate at each angle. The shear rate in the cell was determined from the rotational speed of the driving motor (measured electronically).

The colloidal hematite was obtained from 3M Corp., St Paul, MN; see Figure 4. Dimensions of the hematite

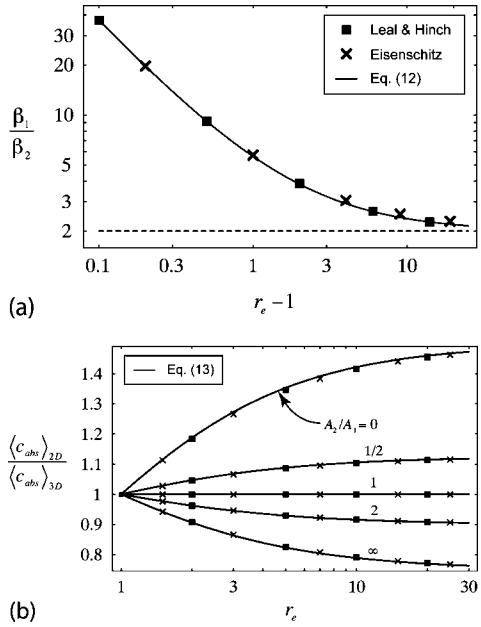

Figure 3. Functional dependence of observables (a) β_1/β_2 and (b) $\langle c_{abs}\rangle_{2D}/\langle c_{abs}\rangle_{3D}$ showing comparison of exact solution using Eisenschitz and Leal and Hinch criteria together with approximate formulas, eqs 12 and 13.

rods are length 320 nm and width 38 nm with an aspect ratio $r_e = 8.4 \pm 1.0$ as measured from Figure 4. Measurements of the hematite rods used here are identical to those we previously reported.[7]

From eq 12, we again note that the ratio of the change in extinction coefficients β_1/β_2 depends solely on the hydrodynamic aspect ratio r_e. Measurement of β_1/β_2 can therefore be used to directly determine the hydrodynamic aspect ratio. Once this is known, the dichroic ratio A_2/A_1 can then be evaluated by measuring $\langle c_{abs}\rangle_{2D}/\langle c_{abs}\rangle_{3D}$. Consequently, the measurement technique follows two distinct stages:

(1) Using *polarized* light, the extinction coefficient $\epsilon_0(\gamma)$ of the quiescent fluid is measured.[14] The shear flow field is then applied and increased until no change in absorbance is observed, thus ensuring the high Peclet number limit is achieved. The extinction coefficient $\epsilon(\gamma)$ as a function of polarization angle γ is then measured. From these two measurements, the change in extinction coefficient $\Delta\epsilon(\gamma) = \epsilon(\gamma) - \epsilon_0(\gamma)$ is determined. Fitting the experimental results for $\Delta\epsilon(\gamma)$ to eq 7 then yields the required ratio β_1/β_2. Note that polarized light is used in both quiescent and sheared samples to ensure no change in optics. The required hydrodynamic aspect ratio r_e is then obtained from eq 12.[15]

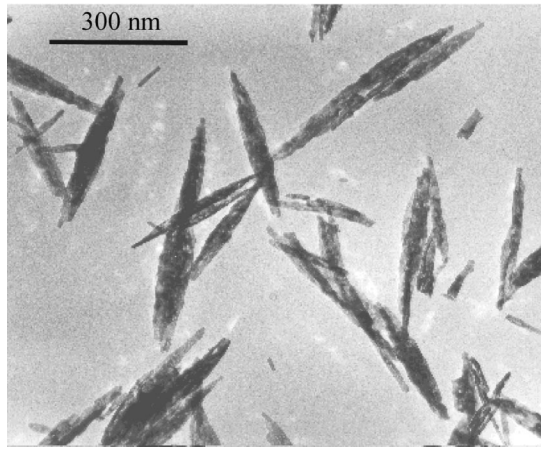

Figure 4. Transmission electron micrograph of the prolate hematite sample, showing the spindle geometry and aspect ratio.

(2) With the hydrodynamic aspect ratio r_e determined, the dichroic ratio A_2/A_1 is obtained by using *unpolarized* light[14] to measure the extinction coefficient of the sample in a sheared and quiescent state. The ratio of these two values is $\langle c_{abs}\rangle_{2D}/\langle c_{abs}\rangle_{3D}$. The dichroic ratio is then determined using eq 13.[15]

We now examine the implications of the above theoretical model and its implementation experimentally. First, from eq 12 we note that the change in extinction coefficient ratio satisfies $\beta_1/\beta_2 \geq 2$, regardless of the hydrodynamic aspect ratio r_e, and is independent of the dichroic ratio A_2/A_1. As such, the critical angle γ_0 that gives zero change in extinction is independent of the optical properties of the rod, *i.e.*, the dichroic ratio. For a rod with a very high hydrodynamic aspect ratio, $r_e \gg 1$, this angle is given simply by

$$\gamma_0 = \tan^{-1}\sqrt{2} \cong 55^\circ$$

Importantly, previous experimental work has used this critical angle to determine the dichroic ratio,[6] with a critical angle of 45° assumed to correspond to a dichroic ratio of unity. The above analysis establishes that this (intuitive) interpretation of measurements is incorrect and that this critical angle is independent of the dichroic ratio. For rods with high aspect ratios, these previous experimental studies yielded a critical angle of $\gamma_0 \sim 60°$, which is consistent with the above theoretical result. Furthermore, our model shows that the critical angle

$$\gamma_0 \geq \tan^{-1}\sqrt{2}$$

and increases with decreasing hydrodynamic aspect ratio r_e.

Figure 5 shows the absorption measurements conducted using unpolarized light for the hematite sample. The shear rate was periodically varied between zero and a finite value and then back to zero. In each cycle, the applied finite shear rate was systematically increased from 0 to 160 s^{-1}. Note that as the shear rate increases from zero, the measured extinction coefficient also increases. Importantly, the measured extinction coefficient at zero shear rate remains unchanged during each cycle indicating that the application of shear does not affect the properties of the dispersion. At high

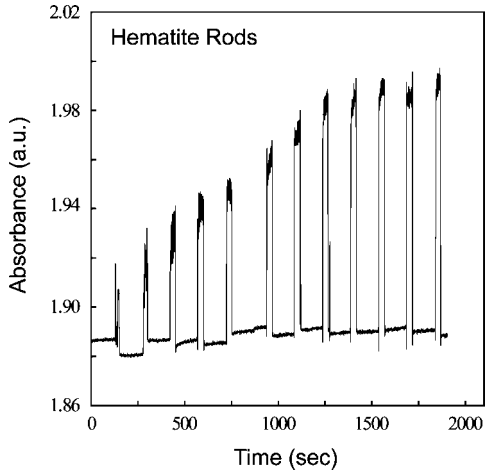

Figure 5. Absorbance for unpolarized light *vs* time for 5 ppm hematite in 80% glycerol/water. Each peak corresponds to an applied shear rate between 0 to 160 s^{-1}.

shear rates, the extinction coefficient plateaus to a constant value and the procedure specified above is implemented in this regime, which corresponds to the high Peclet number limit. An estimate obtained from the dimensions of the particles shows that the Peclet number in this regime exceeds 50.

Identical measurements were also performed using polarized light, which corresponds to stage 1 of the above procedure. The reference extinction coefficient $\epsilon_0(\gamma)$ was obtained with the fluid in a quiescent state. The shear rate was systemically increased until no change in absorption was observable. The extinction coefficient at a range of polarization angles was then measured. The difference between the sheared and unsheared values yielded the required change in extinction coefficient $\Delta\epsilon(\gamma)$, the results of which are given in Figure 6. Also shown in Figure 6 is a fit to eq 7 using a least-squares fitting procedure.[16] Note the good agreement between eq 7 and the measured data. This fitting procedure yielded a value of $\beta_1/\beta_2 = 2.6 \pm 0.1$. Substituting this value into eq 12 gives a hydrodynamic aspect ratio of $r_e = 7.2 \pm 1.2$. This value is to be compared against the independent measurement of $r_e = 8.4 \pm 1.0$ obtained using electron microscopy (see Figure 4), for which excellent agreement is found.[17]

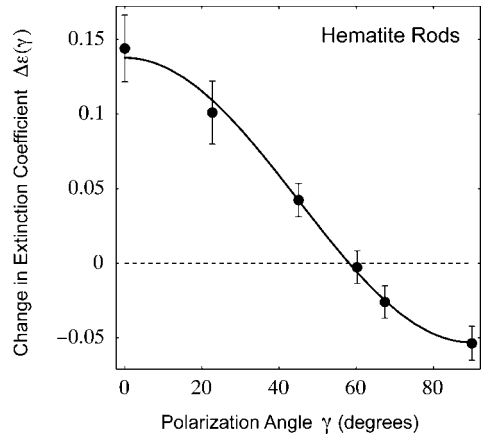

Figure 6. Change in extinction coefficient with polarization angle for hematite rods. Solid line is fit to eq 7. Dashed line is zero change in extinction.

With the hydrodynamic aspect ratio determined as per stage 1, the dichroic ratio is then evaluated by stage 2 using unpolarized light. The measurements for this stage have already been presented in Figure 5. Comparing the extinction coefficients under the application of shear and in a quiescent state yields a value of $\langle c_{abs}\rangle_{2D}/\langle c_{abs}\rangle_{3D} = 1.052 \pm 0.005$. Substituting this value into eq 13 gives a dichroic ratio of $A_2/A_1 = 0.65 \pm 0.05$. This measured value is to be compared to *T*-matrix theory for a spheroid,[18] which yields $A_2/A_1 = 0.57$, obtained using the dimensions above and taking the usual approximation of optical isotropy for hematite[19] with a refractive index of $1.95 + 0.88i$ and 1.44 for the glycerol/water mixture.[20] The difference between the theoretical and experimental results is ~10%, which illustrates the validity of the proposed method. It remains to be seen whether use of the actual (uniaxial[19]) optical properties of our hematite sample in the simulation permits closer agreement between theory and measurement.

In summary, we have presented a technique for simultaneously measuring the optical and geometric properties of small particles using an optical Couette flow apparatus. A commensurate theoretical formalism was developed to determine both the hydrodynamic aspect ratio and the dichroic ratio. This approach circumvents the requirement for independent techniques to measure the optical and geometric properties. The validity of the method was demonstrated by application to a dispersion of hematite nanoparticles. This technique is expected to find application in the characterization of the constituents of advanced materials and thus aid in the fabrication and development of novel devices.

Acknowledgment. This research was supported by the Particulate Fluids Processing Centre of the Australian Research Council and by the Australian Research Council Grants Scheme.

REFERENCES AND NOTES

1. van den Heuvel, M. G. L.; Dekker, C. Motor Proteins at Work for Nanotechnology. *Science* **2007**, *317*, 333–336.
2. Glotzer, S. C.; Solomon, M. J. Anisotropy of Building Blocks and their Assembly into Complex Structures. *Nat. Mater.* **2007**, *6*, 557–562.
3. Peterlin, A. Optical Effects in Flow. *Annu. Rev. Fluid Mech.* **1976**, *8*, 35–55.
4. Fuller, G. G. *Optical Rheometry of Complex Fluids*; Oxford University Press: New York, 1995.
5. Vermant, J.; Yang, H.; Fuller, G. G. Rheooptical Determination of Aspect Ratio and Polydispersity of Nonspherical Particles. *AIChE J.* **2001**, *47*, 790–798.
6. Gason, S. J.; Boger, D. V.; Dunstan, D. E. Rheo-optic Measurements on Dilute Suspensions of Hematite Rods. *Langmuir* **1999**, *15*, 7446–7453.
7. Gason, S. J.; Lester, D.; Yeow, L.; Boger, D. V.; Dunstan, D. E. Predictions of the Change in Extinction Coefficient for Prolate Particles under Shear. *J. Chem. Phys.* **2001**, *115*, 5679–5689.
8. The technique does not make a distinction between geometry and material induced optical anisotropy.

9. Jeffery, G. B. The Motion of Ellipsoidal Particles in a Viscous Fluid. *Proc. R. Soc. London, Ser. A* **1922**, *102*, 161–179.
10. van de Ven, T. G. M. *Colloidal Hydrodynamics*; Academic Press: London, 1989.
11. Leal, L. G.; Hinch, E. J. The Effect of Weak Brownian Rotations on Particles in Shear Flow. *J. Fluid Mech.* **1971**, *46*, 685–703.
12. Eisenschitz, R. The Viscosity of Long Straight Particles in Suspension and its Interpretation by Means of Spatial Strain. *Z. Phys. Chem.* **1931**, *158*, 78–90.
13. Abramowitz, M.; Stegun, I. A. *Handbook of Mathematical Functions*; Dover: New York, 1972.
14. Unpolarized light is used as a probe to measure the dichroic ratio, A_2/A_1, since the baseline absorption of the Couette cell and fluid is typically polarization dependent. This makes comparison of the absolute extinction coefficients at 0 and 90° problematic.
15. Equation 12 can be easily inverted: $r_e = (7 + 4B + \sqrt{16B^2+40B+81})/(8(B - 2))$ where $B \equiv \beta_1/\beta_2$. Equation 13 yields $A_2/A_1 = (2(2 + 3r_e)K - 1 - 9r_e)/(11 + 9r_e - 4(2 + 3r_e)K)$, where $K = \langle c_{abs}\rangle_{2D}/\langle c_{abs}\rangle_{3D}$.
16. *Mathematica* is a registered trademark of, and is available from, Wolfram Research, Inc., 100 Trade Center Dr., Champaign, IL 61820-7237.
17. Note that the influence of sample polydispersity is to modify the shape of the curve specified by eq 7, since β_1/β_2 depends implicitly on this aspect ratio r_e. The effect of this uncertainty on the technique will be small provided sample polydispersity is weak, as demonstrated in the above measurements.
18. Mishchenko, M. L.; Travis, L. D.; Lacis, A. A. *Scattering, Absorption, and Emission of Light by Small Particles*; Cambridge University Press: Cambridge, 2002. FORTRAN code for nonspherical particles in a fixed orientation: http://www.giss.nasa.gov/~crmim/t_matrix.html.
19. Kerker, M.; Scheiner, P.; Cooke, D. D.; Kratohvil, J. P. Absorption Index and Color of Colloidal Hematite. *J. Colloid Interface Sci.* **1979**, *71*, 176–187.
20. Hsu, W. P.; Matijevic, E. Optical Properties of Mondispersed Hematite Hydrosols. *Appl. Opt.* **1985**, *24*, 1623–1630.